ISSN 2320-9984

Volume 13 Issue 4 | December 2025 ISSN: 2320-9984 (Online)

International Journal of Modern Engineering & Management Research

Website: www.ijmemr.org

Subject-Specific Femoral Fracture Risk Prediction: A Multi-Material Finite Element Study of Stance and Fall Conditions

Hussain Waris
MS Scholar
College of Mechanical and Electrical Engineering,
Nanjing University of Aeronautics and Astronautics
Nanjing (210016), China
Email: waris.hussain@nuaa.edu.cn

Tan Zhaolin
MS Scholar
College of Mechanical and Electrical Engineering,
Nanjing University of Aeronautics and Astronautics
Nanjing (210016), China
Email: tanzhaolin@nuaa.edu.cn

Bao Yidong
Associate Professor
College of Mechanical and Electrical Engineering,
Nanjing University of Aeronautics and Astronautics
Nanjing (210016), China
Email: baoyd@nuaa.edu.cn

He Shuangjian
Medical Doctor
Department of Orthopaedics,
The Affiliated Suzhou Hospital of Nanjing University
Medical School, Suzhou (215153), China
Email: hsjian.ok@163.com

Abstract*—Hip fractures among elderly people are associated with elevated mortality rates and significant health burdens. Material assignment in orthopaedics for Finite element analysis is a major challenge that significantly influences simulation results. However, many studies used different methods to assign material properties to the femur model. Therefore, we have adopted three widely used different kinds of material as Homogeneous, Cortical-Cancellous, and Heterogeneous assignment methods to compare the results and influence the outcome of the biomechanical simulation. Early assessment of hip fracture risk is essential for developing preventive approaches aimed at decreasing the incidence of hip fractures among elderly people. Therefore, the second objective of this research is to determine how different falling configurations (FC) increase the hip fracture risk. Six different fall configurations have been used by adjusting the load angle directions (α) on the frontal plane and (β) on the horizontal plane to find the fracture risk. FEA showed that a heterogeneous material model is more consistent in biomechanical simulation. Moreover, the tendency of fracture risk is higher when (α) is 120° and (β) is 45°. The biomechanical simulation results are valid and applicable within the orthopaedic field, supporting their integration into clinical research.*

Keywords:— *FEA, Fracture Risk, biomechanics, simulation, material assignment.*

1. INTRODUCTION

Hip fractures among elderly people frequently result in an increased mortality risk, disability, and subsequent hip fractures, which are mainly caused by osteoporosis. This severe bone disease results in decreased bone mass and an increased fracture risk [1]. It has become a worldwide socioeconomic and substantial health burden [2]. The increased risk of osteoporosis persists for several years subsequently, emphasizing the essential interventions to reduce this risk [3]. Suffering any fracture is associated with heightened mortality risk among men and women, and hip fractures are a significant independent predictor of a higher mortality rate [4].

According to a previous study, hip fractures are predicted to increase to 1.3 million by 2050 [5]. China has the largest population in the world of elderly people, with an increased mortality rate of 13.96% in 1 year due to hip fractures, and the economic impact has grown, with hospitalization costs rising from approximately US$60 million to US$380 million in 2016 [6]-[7]. Therefore, Hip fractures remain a serious concern; early assessment has a considerable reduction in the mortality rate and impacts economic outcomes.

Clinically, Osteoporosis measurement tools are essential for early treatment, monitoring, diagnosis, and hip fracture risk prediction [8]-[9].

Dual-energy X-ray absorptiometry (DXA) is the World Health Organization (WHO)-designated clinical standard for assessing bone mineral density (BMD). It provides a validated and quantitative measure of fracture risk, serving as a primary predictor of osteoporotic hip fracture risk [10]. However, bone mineral density is not the only primary factor in hip fractures; other factors, such as bone strength, bone geometry, and clinical risk factors related to fall postures, may also influence hip fractures [11]. The World Health Organization's FRAX tool estimates the 10-year probability of hip and major osteoporotic fractures but has a key limitation: it does not account for fall risk, which is a significant independent predictor of hip fractures [12]. However, fall is a major risk factor for fracture that has not been included in FRAX, a critical determinant in the aetiology of hip fractures [13]. Conversely, Hip Structural Analysis (HSA) utilizes a 2D model of the femur, which is acquired through Dual-energy X-ray Absorptiometry (DXA), to assess the impact on the bone structure [14]. Hip Structural Analysis (HSA) depends on the reliability of a standardized 2D DXA projection of the femur, which requires precise patient positioning during acquisition [15].

The femur bones possess a highly complex anatomical structure, and their primary functions, including weight-bearing and gait stability, play a significant role in hip fractures [16]. Due to the complex bone structure of the femur, consisting of periosteum, cortical bone, cancellous bone, and the significant differences in their properties [17]. As a result, various researchers in biomechanical simulations of bone models adopt different methods to assign material properties. For instance, studies have assumed the femur bone to be a homogeneous linearly elastic material, viscoelastic material properties of cortical and cancellous bone, and grayscale to adopt the femur bone as heterogeneous, respectively[18]-[20].

Three-dimensional femoral geometry is essential for assessing hip fracture risk. Advanced imaging techniques, particularly Quantitative Computed Tomography (QCT) and Magnetic Resonance Imaging (MRI), enable detailed estimations of volumetric bone mineral density (vBMD), bone geometry, and detection of occult fractures.

However, Magnetic Resonance Imaging (MRI) is a potential tool that excels in soft tissue differentiation, but Quantitative Computed Tomography (QCT) is superior for assessing fracture risk as it quantitatively measures bone density and bone structure [21].

Finite Element Analysis (FEA) is an established computational methodology that enables non-invasive assessment of biomechanical engineering, merging with engineering principles [22]-[23]. The integration of QCT with FEA offers a more reliable numerical approach for assessing hip fracture risk with greater accuracy [24]. Biomechanical studies highlight that 90% of hip fractures are caused by a sideways fall [25]-[26]. However, it is difficult to control falling orientations, which is a necessary assessment of fracture due to sideways falling on the increasing rate of hip fractures. Prior experimental testing demonstrated that changing the loading angle from $0^{\circ}$to 45° measured from the neck axis of the femur on the horizontal plane 26% reduction in load-

bearing capacity, equal to bone degradation over 2–3 years of aging [25]. A comparable study indicates that varying the loading angle maximum of 30° from the femoral neck axis leads to a 24% reduction in femoral strength, equivalent to twenty-five years of bone aging [26]. In studies, the fracture load was determined with varying angles on different planes [19]. However, Fracture load might not be a completely reliable way to predict the risk of fracture, because when a person falls from standing height, the actual force they experience can vary. Moreover, there is currently a lack of comprehensive comparisons and systematic studies on the impact of different material assignment strategies on the results of biomechanical finite element simulations in orthopaedics.

Therefore, we have adopted three widely used material types as Homogeneous, Cortical -Cancellous, and Heterogeneous assignment methods to compare the results and influence the outcome of the biomechanical simulation. The results of the biomechanical study were compared using a single-leg-stance configuration. Furthermore, early assessment of hip fracture risk plays a critical role in developing preventive measures aimed at reducing the incidence of hip fractures among the elderly. Therefore, the second objective of this research is to determine how different falling configurations (FC) increase the hip fracture risk. Six different fall configurations have been used by adjusting the load angle directions (α) on the frontal plane and (β) on the horizontal plane to find the fracture risk shown in Figure 5.

2. FEMUR ANATOMICAL STRUCTURE

The femur is the longest and strongest bone in the human body, connecting the body to the lower limbs at the knee joint, supporting body weight, and facilitating movement. The proximal femur includes the femoral head, which articulates with the pelvis to form the hip joint, essential for various movements. The femoral neck connects the head to the femoral shaft and is vital for alignment and load distribution. The trochanteric region serves as an attachment site for muscles and ligaments, enhancing stability. The femur's structure consists of a dense cortical outer layer transitioning to a spongy trabecular core for reduced weight and enhanced load distribution. The femoral shaft withstands significant forces, ensuring efficient force transmission from hip to knee. Osteoporotic fractures commonly occur in the proximal femur due to low bone mineral density, emphasizing the need to understand the femur's geometry for assessing fracture risk and different fractures. Figure 1. depicts that hip fractures are subdivided into different types [27]. The detailed anatomical structure of the femur bone shown in Figure 2.

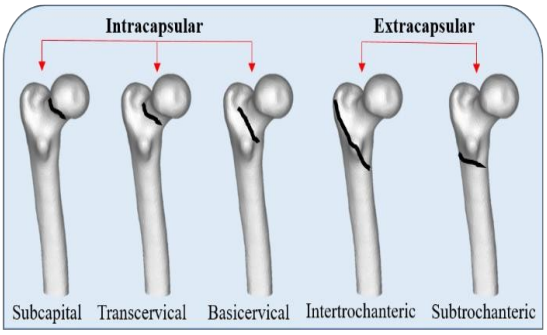

Figure 1: Types of Hip fractures.

3. MATERIALS AND METHODS

This section outlines the essential components of the study, including the equipment and software tools used, details of the experimental/research subject, and the reconstruction of the 3D femur FE model. Furthermore, it explains the meshing and material assignment process, the chosen failure measure, and the applied loading and boundary conditions. It also describes sensitivity analysis to assess the impact of varying loading angles.

A. Equipment and Software Tools

For this research, a high-resolution 64-slice spiral CT scanner manufactured by Siemens, Germany, was used to obtain detailed imaging data of the femur. The CT scanning took place at Suzhou Science and

Technology City Hospital, providing a highly accurate representation of actual anatomy. The acquired DICOM data were processed and analysed using advanced medical imaging and engineering software tools. Mimics Research 21.0 was utilized for segmentation and three-dimensional reconstruction of the bone finite femur model. The bone femur 3D model was further refined in Geomagic Wrap to ensure smoothness and accuracy. HyperMesh 2019 was employed for mesh generation and pre-processing, while Abaqus 2024 served as the core finite element analysis platform for simulating loading and fall configurations. These tools collectively ensured precision and reliability in the simulation workflow.

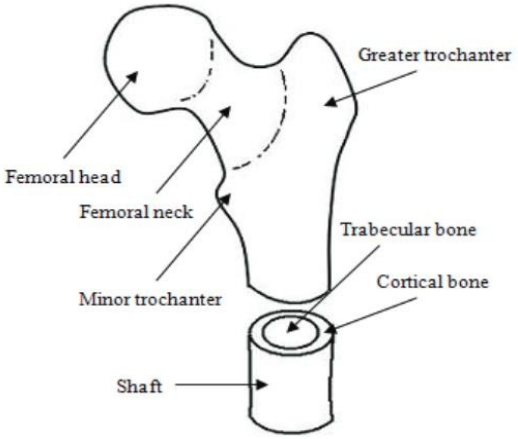

Figure 2 : Structure of the Femur bone.

B. Experimental/Research Subject

A healthy elderly female volunteer was selected as the experimental subject. The participant had no prior history of internal or surgical diseases, limb disabilities, or trauma, and she had a body weight of approximately 60 kg. To ensure high- resolution imaging of the femoral structure, bilateral upper femoral CT imaging was utilized using a 64-slice spiral CT scanner from Siemens, Germany. The scanning protocol was carefully designed with a slice thickness of 1 mm and an inter-slice spacing of 1 mm to acquire detailed bone morphology. The scanning range extended from a point 10 cm above the apex of the greater trochanter down to the plane of the knee joint. The data for the left femur was selected as the primary specimen for modelling and simulation. All series of CT image data was stored in Digital Imaging and Communications in Medicine (DICOM) format for further analysis and 3D model reconstruction. The experimental protocol conforms with the informed consent of the volunteer and complies with the relevant ethical requirements of Suzhou Science and Technology City Hospital. Figure 3. shows the 3D reconstruction process of the proximal femur from a DICOM file.

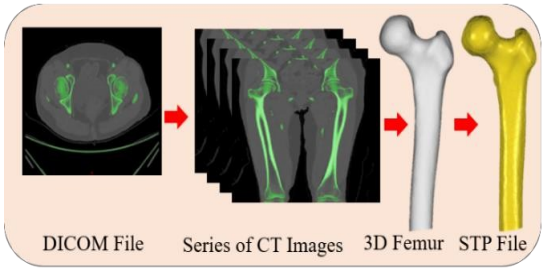

Figure 3: Three-dimensional reconstruction process of the femoral model from CT data

C. 3D Femur Model Reconstruction

The DICOM file was imported into the widely used medical image processing software, Mimics Research 21.0. The femur was carefully segmented from anatomical structures such as the tibia, pelvis, fat, and muscle using the default "Bone(CT)" threshold to segment the femur. A 3D reconstruction of the left femoral model was performed through operations such as region growing (Region Grow), split masks (Split Masks), smart filling (Smart Fill), calculating entities (Calculate Part), and smoothing (Smooth). Later, the 3D reconstructed model of the femur was imported into Geomagic Wrap software in Standard Tessellation Language (STL) format, and the left femur model was created through steps such as meshing, deleting, trimming, and filling holes. The model was optimized by operations such as fitting curved surfaces and saved as a STEP format file.

D. Meshing and Material Assignment

The 3D model was imported into HyperMesh (Altair, USA) software, an advanced meshing pre-processor suite, in

STEP format. The 3D femur mesh was created using the element type C3D10, a tetrahedral mesh. Through the verification and analysis of mesh convergence, considering the comprehensive factors of calculation time and accuracy, the element size was chosen to be 1.8 mm. In this study, for all the simulations of 3D femoral models, meshing was done with an element size of 1.8 mm, keeping the same boundary and loading conditions. Afterwards, the meshed model was imported into Mimics software for material assignment. The bone model was adopted to be homogeneous, with a Young's Modulus of 16.7GPa and a Poisson's ratio of 0.3. The 3D femur was divided into compact (cortical) bone and cancellous (trabecular) bone with the Boolean divide operation in SolidWorks, which considers the femur as a combination of compact femur bone and trabecular femur bone materials. The elastic modulus of cortical bone was 16.7GPa, the elastic modulus of cancellous bone was 1.55GPa, and the Poisson's ratio was 0.3 for both models. Figure 4 shows three material models considered in this study. For heterogeneous material, femur bone material was assigned by applying Mimics' default empirical formulas as follows:

$$\rho = -13.4 + 1017 * \mathrm{GV} \quad \text{..... (1)}$$

$$E = -388.8 + 5925 * \rho \quad \text{..... (2)}$$

$$\nu = 0.3 \quad \text{..... (3)}$$

Where ρ, GV, and ν are density, gray value, and Poisson's ratio, respectively.

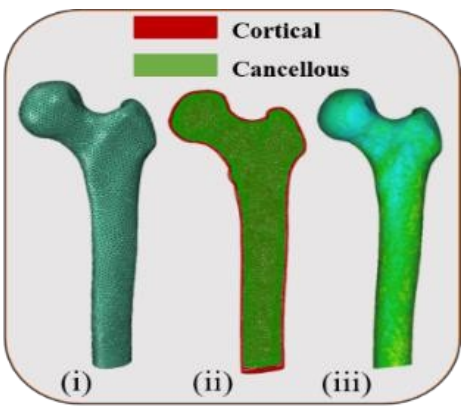

Figure 4: Material models (i) Homogenous (ii) Cortical - Cancellous (iii) Heterogeneous.

E. Failure Measure

In this study, we performed linear finite element analysis (FEA) as experimental studies have shown that the femur bone exhibits linear-elastic behaviour under falls and stance load configurations up to failure, demonstrated through testing cadaveric femurs and measuring strain on the bone surface [28]. The choice of failure criterion has a considerable impact on FEA's ability to predict hip fracture risk. For each loading condition, the study used the maximum strain criteria to determine fracture risk (FR), which was validated against in vitro experimental data and successful in vivo applications. ε^{T}_{max} and ε^{C}_{max} represent the maximum tensile and compressive principal strains, respectively. in (4) and (5), respectively [29].

$$FR = \frac{\varepsilon^{T}_{max}}{0.0073} \quad (4)$$

$$FR = \frac{|\varepsilon^{c}_{max}|}{0.0104} \quad (5)$$

Table 1: FALL CONFIGURATIONS (FC)

Fall Configurations	α (deg.)	β (deg.)
FC1	60	-30
FC2	90	-15
FC3	120	0
FC4	60	15
FC5	90	30
FC6	120	45

F. Loading and Boundary Condition

For a precise Finite Element (FE) analysis during single-leg stance and fall configurations, loading and boundary conditions are necessary in the FE model. To simulate a single-leg stance configuration, 2.5 times of body weight patient-specific load was coupled on the superior head of the femur perpendicular to the femur shaft axis [30], and the distal condyle was fixed in all directions based on experiments, as shown in Figure 5.

$$F_{Stance} = 2.5w\ (N) \quad (6)$$

Where w is the weight of the research subject. To simulate fall conditions, the loading angles (α) on the frontal plane and the angles (β) on the horizontal plane are considered. For all falling configurations, the amount of load is calculated as per equation (7) [30].

$$F_{fall} = 8.25w\left(\frac{h}{70}\right)^{1/2} \ (N) \qquad (7)$$

Where w represents the weight and h represents the height of the research subject, respectively. The fall configurations (FC) were mimicked by varying the adduction angle (α) and rotation angle (β) shown in Figure 5.

In the finite element (FE), the 6 fall configuration (FC) was simulated by the adduction angle (α) and femur rotation angle (β). Each FC has a unique angle combination; the adduction angle (α) and rotation angle (β) were varied, α = [60°, 90°, 120°] with β = [–30°, –15°,0°] respectively. In the second case, the adduction angle (α) and rotation angle (β) were varied, α = [60°, 90°, 120°] with β = [15°, 30°, 45°] respectively. Table 1 shows FC. For all falling conditions, the distal condyle can rotate in the y-axis but is fixed in the other axis, representing the pivot joint, and the falling impact force was applied perpendicular to the greater trochanter [31]-[32].

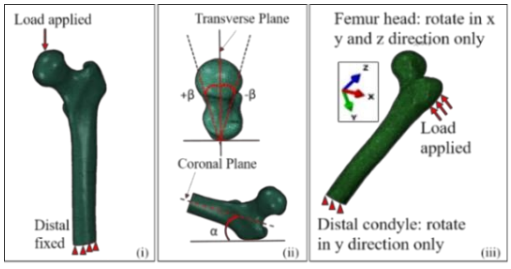

Figure 5. (i) Stance Configuration (ii) Fall Configurations loading angle (iii) Loading and boundary conditions.

IV. RESULTS AND DISCUSSION

This study compared the three widely used material assignment models conducted in Abaqus 2024. The Von Misses distribution in femurs was obtained for the single-leg-stance loading case. In addition, the stress distribution of each model is realistically different shown in Figure 6. Von Mises stress distribution of homogenous and cortical-cancellous models is mainly higher at the femoral shaft and more uniform due to constant material properties. On the other hand, the maximum von Mises stress distribution at the neck of the femur by MIMICS-based formula grayscale material assignment. In the heterogeneous material mapping, each region of bone is classified based on its grayscale values, which correspond to realistic material properties in orthopaedics.

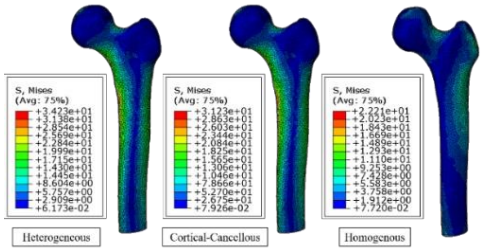

Figure 6. Cloud mapping of femur Von Mises stress distribution of three materials.

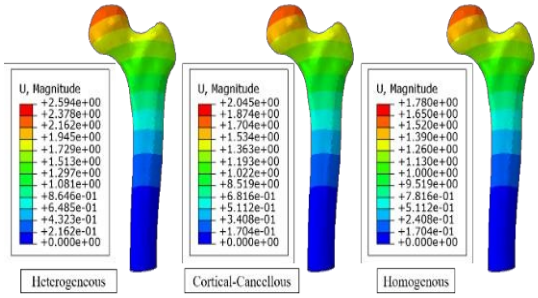

Fig. 7. Cloud mapping of femur displacement distribution of three materials.

Figure 7 shows the displacement of Homogenous, Cancellous- Cortical, and heterogeneous (grayscale value) MIMICS Empirical formula for the single-leg-stance loading condition. The displacement value of cortical-cancellous and heterogeneous properties is more consistent. While the displacement varies, with homogeneous is 33.69% than for heterogeneous material properties. Figure 8. shows von Mises stress and displacement of Homogenous, Cancellous -Cortical, and heterogeneous (gray value) MIMICS Empirical formula for the single-leg-stance loading condition. Load applied during

single-leg stance configuration stress values of homogenous Cancellous-Cortical and heterogeneous (grayscale value) MIMICS formula von Mises stress are 22.1 MPa, 31 MPa, and 34 MPa, respectively. The output values of all three single-leg stance models are within a reasonable range. The maximum stress was at the Transcervical fracture region and the intertrochanteric fracture region of the femur. Furthermore, the stress concentration values derived from the homogeneous material model and the Mimics-based formula vary by nearly 35%. Additionally, the difference between the result values of the cortical-cancellous model and the Mimics-based formula is approximately 9.6%. Moreover, stress cloud mapping of the three models is significantly different. The maximum stress distribution of the homogenous and Cortical-Cancellous model is in the femoral shaft. On the other hand, the MIMICS-based model exhibits stress concentration in the neck of the femur bone, as shown in Figure 6. The neck region of the femur is at a higher risk of fractures compared to the femoral shaft of the femur bone due to its complex geometry and reduced cortical thickness [27]. Therefore, MIMICS-based material assignment is more consistent with bone properties.

The strain distribution was analysed in Abaqus for six sideways fall configurations using heterogeneous material. The analysis clearly demonstrates that there is a higher strain concentration in the femur neck region than in the femoral shaft. By varying the angle (α) (on the frontal plane) from 60° to 120°, higher tensile strains were noted in the proximal femoral neck and intertrochanteric regions. Furthermore, the angle (β) (on the horizontal plane), varied from –15° to 45°, was found to have a critical influence on strain generation. Variation of compressive and tensile at each fall configuration is shown in Table 1. The tendency of tensile strain concentration and compressive strain concentration are higher in the posterior as compared to the anterior fall configurations shown in Figure 9. The compressive strain concentration on the upper surface of the femoral neck region increased with a larger angle (β), with the maximum compressive strain observed at 45°. This study provides a detailed assessment of sideways falls by varying the loading angle (α) on the frontal plane and the angle (β) on the horizontal plane. The angle (α) was varied at 30° intervals, and the angle (β) was varied at 15° intervals for both anterior and posterior fall configurations. When the α or β angles were altered in this study, significant changes in the strain distribution of the femur were observed. The femoral neck and intertrochanteric regions consistently exhibited higher principal strain compared to other regions, as shown Figure 10., primarily due to the relatively thin cortical bone in the femoral neck, which makes it mechanically more sensitive under loading. This reduced cortical thickness increases stress concentration and creates a higher likelihood of fracture initiation. Similarly, the intertrochanteric region showed elevated strain as it represents a transitional zone between cortical and cancellous bone. Overall, both tensile and compressive strains were predominantly localized in the proximal femur, particularly in the neck and intertrochanteric regions. These findings explain why fractures most frequently occur in these areas and support existing clinical evidence regarding their vulnerability. Consequently, variations in geometric parameters such as α and β angles should be carefully considered in biomechanical analyses and surgical planning to better predict and prevent proximal femoral fractures.

Medical imaging and medical engineering have significantly advanced the field of orthopaedics, resulting in considerable improvements in clinical diagnosis and treatment compared to the 20th century. However, computer-aided technology and FEA provide accurate tools for calculation and simulation, overcoming these limitations. Therefore, this extensive research study was conducted on the biomechanical properties of human bone.

through the comparison of three different materials femur models, it is found that all three models have von Mises stress within a reasonable range. Figure 8. It is evident that the maximum stress obtained by homogenous and cortical- cancellous models is mainly distributed in the femur shaft. In contrast, the stress response by the heterogeneous material model is mainly in the neck of the femur, which is more realistic. Fig 6. The von Mises stress obtained in this study is validated with prior studies [14]. The concentration of strain at different Fall configurations. Figure 10. evident that femoral fractures mainly depend on the variation of (α) on the frontal plane and (β) on the horizontal plane; the risk of femoral neck and intertrochanteric region increases when both angles are at maximum. Therefore, Prior studies showed that the tendency of fractures is highest when α 120° and (β) 45° shown in Figure 9. [25]-[33].

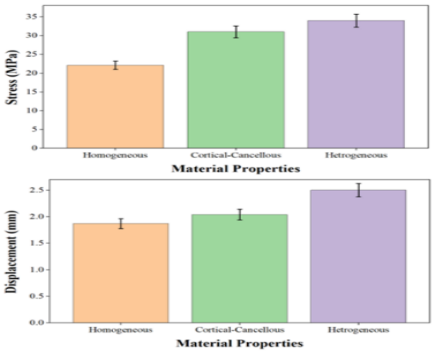

Figure 8: Comparison of von Mises stress and Displacement for three material models.

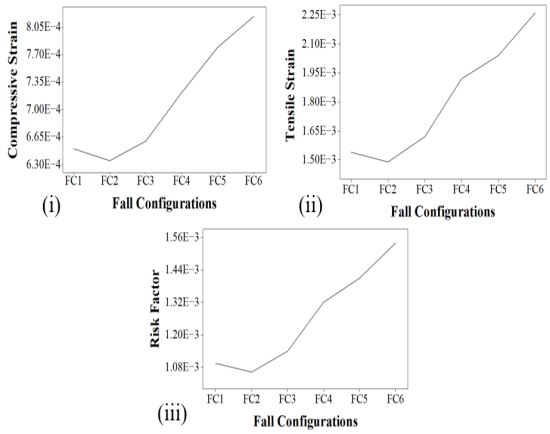

Figure 9: Variation of (i) compressive strain, (ii) tensile strain, and (iii) risk factor with respect to fall configurations (FC).

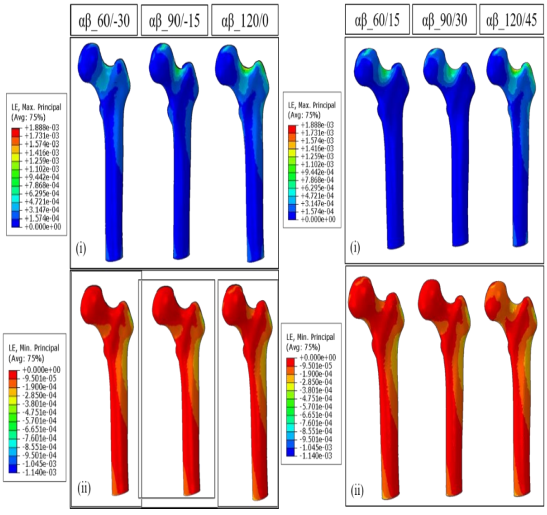

Figure 10: Maximum tensile strain (i), Maximum compressive strain (ii) distribution at different fall configurations (FC).

5. CONCLUSION

Hip fractures remain one of the most critical health concerns in the elderly, often leading to severe disability and reduced quality of life. In this study, Assessing Hip Fracture Risk: FEA of Stance and Fall Conditions Using Three Material Models, the study aimed to explore how material assignment and loading direction influence the responses and fracture risk. This study comprises two purposes; the primary objective of this research was to analyse the influence of material assignment on the results of biomechanical simulation. To investigate the effect of material assignment, three material models were used as homogeneous, cortical-cancellous, and heterogeneous (MIMICS-based grayscale) for the single-leg stance configuration. The second aim of this research was to investigate the impact of loading directions on the fracture risk (FR) obtained via FEA. The strain-based criterion was used to obtain the strain distribution. The following conclusions have been drawn from this study:

1. The comparison of three widely used materials models, homogenous, cortical cancellous, and heterogeneous (grayscale), revealed significant variations in von Mises stress, 22.1 MPa, 31

MPa, and 34 MPa, respectively. The difference in von Mises stress between the homogeneous material model and the MIMICS-based approach was approximately 35%, while the cortical-cancellous model exhibited a deviation of about 9.6% compared to the MIMICS-based results.

2. The displacement values of cortical-cancellous and heterogeneous properties were more consistent. While the displacement varies, with homogeneous was 33.69% than for heterogeneous material properties. Results are evident that a heterogeneous mimics-based model is more realistic with bone properties and can capture the complex variations in density and stiffness, leading to more accurate stress and displacement distribution in biomechanical simulations.

3. The concentration of strain in the femur varies for each specific loading angle in the fall configuration (FC). As the adduction angle (α) increases from 60° to 120° and the rotation angle (β) increases from –30° to 45°, the fracture risk also increases, progressing from FC1 to FC6.

The findings of this study provide significant insights into the fracture risk of the hip, with applications in clinical diagnosis and protective strategies such as hip protectors. Early prediction can also decrease the fracture rate of the hip by guiding preventive health strategies. Future research should focus on heterogeneous materials, validating simulations with clinical data, including diverse populations, and investigating time-dependent bone remodelling to strengthen FEA as a predictive tool in orthopaedics.

REFERENCES:

[1] A. Aldieri, M. Terzini, A. L. Audenino, C. Bignardi, and U. Morbiducci, combining shape and intensity dxa-based statistical approaches for osteoporotic HIP fracture risk assessment, *Comput. Biol. Med.*, vol. 127, p. 104093, Dec. 2020.

[2] L. Cui, M. Jackson, Z. Wessler, M. Gitlin, and W. Xia, Estimating the future clinical and economic benefits of improving osteoporosis diagnosis and treatment among women in China: a simulation projection model from 2020 to 2040, Arch. *Osteoporos.*, vol. 16, no. 1, p. 118, Aug. 2021.

[3] F. F. Lyu, V. Ramoo, P. L. Chui, C. G. Ng, and Y. Zhang, Prevalence rate of primary osteoporosis in China: a meta- analysis, *BMC Public Health*, vol. 24, no. 1, p. 1518, June 2024.

[4] M. Piirtola, T. Vahlberg, M. Löppönen, I. Räihä, R. Isoaho, and S.-L. Kivelä, Fractures as predictors of excess mortality in the aged—A population-based study with a 12-year follow-up, *Eur. J. Epidemiol.*, vol. 23, no. 11, pp. 747–755, Nov. 2008.

[5] X. F. Gong *et al.*, Current status and distribution of hip fractures among older adults in China, Osteoporos. *Int.*, vol. 32, no. 9, pp. 1785–1793, Sept. 2021.

[6] Z. Cui *et al.*, Age-specific 1-year mortality rates after hip fracture based on the populations in mainland China between the years 2000 and 2018: a systematic analysis, *Arch.* Osteoporos., vol. 14, no. 1, p. 55, May 2019.

[7] C. Zhang *et al.*, Incidence of and trends in hip fracture among adults in

urban China: A nationwide retrospective cohort study, PLOS *Med.*, vol. 17, no. 8, p. e1003180, Aug. 2020.

[8] A. S. Areeckal, M. Kocher, and S. D. S., Current and Emerging Diagnostic Imaging-Based Techniques for Assessment of Osteoporosis and Fracture Risk, *IEEE* Rev. *Biomed. Eng.*, vol. 12, pp. 254–268, 2019.

[9] M. Ito, Clinical Diagnostic Tools of Osteoporosis: Vertebral Fracture Assessment and Measurement of Bone Mineral Density (BMD), in *Osteoporotic Fracture and Systemic Skeletal* Disorders*: Mechanism, Assessment, and Treatment*, H. E. Takahashi, D. B. Burr, and N. Yamamoto, Eds., Singapore: Springer Singapore, 2022, pp. 163–176.

[10] G. M. Blake and I. Fogelman, The clinical role of dual energy X- ray absorptiometry, *Osteoporosis*, vol. 71, no. 3, pp. 406–414, Sept. 2009.

[11] P. Geusens, T. Van Geel, and J. Van Den Bergh, can hip fracture prediction in women be estimated beyond bone mineral density measurement alone, *Ther. Adv. Musculoskelet. Dis.*, vol. 2, no. 2, pp. 63–77, Apr. 2010.

[12] M. Chakhtoura *et al.*, Systematic review of major osteoporotic fracture to hip fracture incidence rate ratios worldwide: implications for Fracture Risk Assessment Tool (FRAX)-derived estimates, *J. Bone Miner. Res.*, vol. 36, no. 10, pp. 1942–1956, Dec. 2020.

[13] I. T. Liu, F. W. Liang, S. T. Wang, C. M. Chang, T. H. Lu, and C. H. Wu, the effects of falls on the prediction of osteoporotic fractures: epidemiological cohort study, *Arch. Osteoporos.*, vol. 16, no. 1, p. 110, July 2021.

[14] H. Kheirollahi and Y. Luo, Assessment of Hip Fracture Risk Using Cross-Section Strain Energy Determined by QCT-Based Finite Element Modeling, *BioMed Res. Int.*, vol. 2015, pp. 1–15, 2015.

[15] R. H. J. A. Slart *et al.*, Updated practice guideline for dual-energy X-ray absorptiometry (DXA), *Eur. J. Nucl. Med. Mol.* Imaging, vol. 52, no. 2, pp. 539–563, Jan. 2025.

[16] Chang A, Breeland G, Black AC, et al. Anatomy, Bony Pelvis and Lower Limb: Femur. [Updated 2023 Nov 17]. In: StatPearls. Treasure Island (FL): StatPearls Publishing; 2025.

[17] S. M. Ali Banijamali, R. Oftadeh, A. Nazarian, R. Goebel, A. Vaziri, and H. Nayeb-Hashemi, Effects of Different Loading Patterns on the Trabecular Bone Morphology of the Proximal Femur Using Adaptive Bone Remodeling, J. Biomech. Eng., vol. 137, no. 011011, Jan. 2015.

[18] P. K. Satapathy, B. Sahoo, L. N. Panda, and S. Das, Finite element analysis of functionally graded bone plate at femur bone fracture site, *IOP Conf. Ser. Mater. Sci. Eng.*, vol. 330, p. 012027, Mar. 2018.

[19] R. Zhang, H. Gong, J. Fang, Z. Gao, and D. Zhu, prediction of proximal femoral fracture in sideways falls using nonlinear dynamic finite element analysis, *J. Mech. Med. Biol.*, vol. 14, no. 02, p. 1450026, Apr. 2014.

[20] L. Zhou, L. Wang, R. Xu, Y. Bao, S. He, and X. Xu, Finite element analysis of femoral intertrochanteric fracture treated with intramedullary nail with different lateral wall classifications, *Chin. J. Tissue Eng.*

Res., vol. 27, no. 29, p. 4652, 2023.

[21] E. Boehm, E. Kraft, J. T. Biebl, B. Wegener, R. Stahl, and I. Feist-Pagenstert, Quantitative computed tomography has higher sensitivity detecting critical bone mineral density compared to dual-energy X-ray absorptiometry in postmenopausal women and elderly men with osteoporotic fractures: a real-life study, *Arch. Orthop. Trauma Surg.*, vol. 144, no. 1, pp. 179–188, Jan. 2024.

[22] D. Moratal, *Finite Element Analysis*. BoD – Books on Demand, 2010.

[23] A. Erdemir, T. M. Guess, J. Halloran, S. C. Tadepalli, and T. M. Morrison, Considerations for reporting finite element analysis studies in biomechanics, *J. Biomech.*, vol. 45, no. 4, pp. 625–633, Feb. 2012.

[24] H. Mosleh, G. Rouhi, A. Ghouchani, and N. Bagheri, Prediction of fracture risk of a distal femur reconstructed with bone cement: QCSRA, FEA, and in-vitro cadaver tests, *Phys. Eng. Sci. Med.*, vol. 43, no. 1, pp. 269–277, Mar. 2020.

[25] C. M. Ford, T. M. Keaveny, and W. C. Hayes, the effect of impact direction on the structural capacity of the proximal femur during falls, *J. Bone Miner. Res.*, vol. 11, no. 3, pp. 377–383, 1996.

[26] T. P. Pinilla, K. C. Boardman, M. L. Bouxsein, E. R. Myers, and W. C. Hayes, Impact direction from a fall influences the failure load of the proximal femur as much as age-related bone loss, *Calcif. Tissue Int.*, vol. 58, no. 4, pp. 231–235, Apr. 1996.

[27] J. Thevenot, Biomechanical assessment of hip fracture: development of finite element models to predict fractures.

[28] M. M. Juszczyk, L. Cristofolini, and M. Viceconti, the human proximal femur behaves linearly elastic up to failure under physiological loading conditions, *J. Biomech.*, vol. 44, no. 12, pp. 2259–2266, Aug. 2011.

[29] E. Schileo, F. Taddei, L. Cristofolini, and M. Viceconti, Subject- specific finite element models implementing a maximum principal strain criterion are able to estimate failure risk and fracture location on human femurs tested *in vitro*, *J. Biomech.*, vol. 41, no. 2, pp. 356–367, Jan. 2008,

[30] T. Yoshikawa *et al.*, Geometric structure of the femoral neck measured using dual-energy X-ray absorptiometry, *J. Bone Miner. Res.*, vol. 9, no. 7, pp. 1053–1064, J\50090713.

[31] Z. Altai, M. Qasim, X. Li, and M. Viceconti, the effect of boundary and loading conditions on patient classification using finite element predicted risk of fracture, *Clin. Biomech.*, vol. 68, pp. 137–143, Aug. 2019.

[32] S. N. Robinovitch, W. C. Hayes, and T. A. McMahon, Prediction of Femoral Impact Forces in Falls on the Hip, *J. Biomech. Eng.*, vol. 113, no. 4, pp. 366–374, Nov. 1991.

[33] R. Awal and T. R. Faisal, Multiple Regression Analysis of Hip Fracture Risk Assessment Via Finite Element Analysis, *J. Eng. Sci. Med. Diagn. Ther.*, vol. 4, no. 1, p. 011006, Feb. 2021.